УДК 523.985.3

НАБЛЮДЕНИЯ КВАЗИПЕРИОДИЧЕСКОГО ЭНЕРГОВЫДЕЛЕНИЯ КАК РЕЗУЛЬТАТА ВОЗБУЖДЕНИЯ МГД-ОСЦИЛЛЯЦИЙ В СИСТЕМЕ ВСПЫШЕЧНЫХ ПЕТЕЛЬ

И.В. Зимовец, А.Б. Струминский

OBSERVATIONS OF QUASI-PERIODIC ENERGY RELEASE AS A RESULT OF EXITAFION OF MHD OSCILLATIONS IN A SYSTEM OF FLARE LOOPS

I.V. Zimovets, A.B. Struminsky

В работе исследуется солнечная вспышка 20 октября 2002 г. Вспышка сопровождалась квазипериодическими пульсациями (КПП) как теплового, так и нетеплового жесткого рентгеновского излучения, наблюдавшегося космическим аппаратом RHESSI в диапазоне энергий 3–50 кэВ. Анализ временных профилей темпа счета RHESSI жесткого рентгена различных энергий, выполненный с помощью построения периодограмм Ломба, позволил выявить два статистически значимых периода колебаний: примерно 16 и 36 с. Пульсации с периодом 36 с наблюдались только у нетеплового жесткого рентгена в импульсной фазе вспышки. Пульсации с периодом 16 с были более выражены у теплового жесткого рентгена и наблюдались как в импульсной фазе вспышки, так и в фазе спада. Анализ изображений вспышечной области, определенные периоды пульсаций излучения и оцененные физические параметры петель вспышечной области позволяют интерпретировать наблюдаемые КПП как результат возбуждения МГД-осцилляций в нескольких пространственно разнесенных вспышечных петлях.

In this work we investigate the solar flare of 20 October 2002. The flare was accompanied by quasi-periodic pulsations (QPP) of both thermal and nonthermal hard X-ray emissions (HXR) observed by RHESSI in the 3–50 keV energy range. Analysis of the HXR time profiles in different energy channels made with the Lomb periodogram indicates two statistically significant time periods: about 16 and 36 seconds. The 36-s QPP were observed only in nonthermal HXR in the impulsive phase of the flare. The 16-s QPP were more pronounced in thermal HXR and were observed both in the impulsive and decay phases of the flare. Imaging analysis of the flare region, the determined periods of the QPP and the estimated physical parameters of loops in the flare region allow us to interpret the observed QPP as a result of excitation of MHD oscillations in different flaring loops.

1. Introduction

Electrons accelerated during solar flares generate nonthermal HXR and microwave emissions in the solar atmosphere as a result of their Coulomb collisions with ambient plasma and interaction with magnetic field, respectively. Often, the light curves of nonthermal HXR and microwave emissions in large solar flares consist of multiple pulses with different duration from less than one second up to several minutes (e.g., [1] and references therein), indicating many episodes of acceleration of electrons possibly in different places of the flare regions, since the majority of these flares are accompanied by formation of arcades of many flare loops and by the HXR emission generated in different flare loops (e.g., [2, 3, 4]). It was suggested that flares consist of a number of Elementary Flare Bursts (EFB) that may result from collisions between current-carrying loops (see [3] and references therein).

More rarely, light curves of nonthermal HXR and microwave emissions show apparent quasi-periodic pulsations (QPP; see, e.g., [1, 5, 6] for a review). They may indicate the presence of some quasi-periodic processes of electron acceleration. RHESSI imaging observations in the HXR range are used to show that this quasi-periodic electron acceleration, at least in some flares, occurs in different flare loops, not in a single one [7]. In this case the observed quasi-periodicity could be no more than a chance owing to similar physical conditions in successively bursting flare loops, returning us to the idea of multiple EFB due to current-carrying loops coalescences or due to the presence of multiple spatially separated null-points in flare regions in which stored magnetic energy can be released. But in principle, it is possible to implement a model proposed in [8] to explain the QPP in the latter case by the quasi-periodic reconnection in different null-points due to fast magnetoacoustic oscillations in nearby non-flare loops.

On the other hand, it was theoretically suggested that the QPP could be produced inside a single vibrating flare loop by the quasi-periodic modulation of the spectrum of nonthermal electrons through the betatron acceleration [9] or by the quasi-periodic modulation of efficiency of trapped nonthermal electrons to precipitate into lower heights with the larger plasma density and stronger magnetic field (in particular, the sausage mode is a good candidate for this) [10]. Indeed, some imaging observations of QPP in the microwave range made using the Nobeyama Radioheliograph with the sufficient spatial resolution were interpreted in terms of the global sausage mode of flaring loop oscillations [11]. Other imaging observations of QPP but without sufficient spatial resolution together with the analysis of the time periods of the QPP allowed interpreting QPP in terms of the flare loop oscillations (e.g., [12, 13]). Different modes of oscillations in coronal loops were actually found by TRACE and SOHO spacecraft in the range of the extreme ultraviolet radiation (e.g., [1, 6] and references therein), making loop oscillations a natural way to explain QPP of electromagnetic emission in flares. However, despite the large number of papers published on the flare QPP, their nature is still not fully understood. Further imaging analysis of flares with the QPP is required.

In this work, we investigate the solar flare of 20 October 2002. The light curves of its thermal and nonthermal HXR emission detected by RHESSI clearly indicate presence of the QPP with two significant time periods of 14–17 and 36–37 s.

2. Data and Instrumentations

1. The Reuven Ramaty High-Energy Solar Spectroscopic Imager (RHESSI) is used to detect solar X-rays. The time resolution of RHESSI is about 4 s. RHESSI can detect X-rays with energy resolution of about 1 keV and with spatial resolution of about 2.3 arcsecs in the 3–100 keV range.

2. Three-second data sets of X-ray emission detected by the X-Ray Sensor (XRS) onboard the GOES-10 satellite in two energy channels (1–8 and 0.5–4 A) are used. Unfortunately, the Solar X-ray Imager onboard the GOES-12 satellite did not produce images of the Sun during the flare.

3. One-second ground-based radio data (flux) are obtained from two observatory of the Radio Solar Telescope Network (RSTN) – the Sagamore Hill Radio Observatory (USA) and the San Vito Solar Observatory (Italy) – at standard frequencies of 245, 410, 610, 1414, 2695, 4995, 8800, and 15400 MHz. Unfortunately, these observatories do not make imaging observations of the Sun. The Nobeyama Radioheliograph, who can make images of the Sun in the microwave range, was in the night time during the flare.

4. Full-disk images made in Fe XII lines (about 195 A) by the Extreme-Ultraviolet Imaging Telescope (EIT/SOHO) with the spatial resolution of 2.62 arcsecs and the cadence of about 12 minutes are used to determine configuration of magnetic loops in the flare region. Unfortunately, TRACE, which has better spatial resolution and fewer cadence, observed different active regions during this flare.

5. Level 1.8 full-disk photospheric line-of-sight magnetograms made by MDI/SOHO with the spatial resolution of about 2 arcsecs are used to determine magnetic field configuration and the magnetic inversion lines in the flare region and to roughly estimate magnetic fields in flare loops.

3. Observations

3.1 Time and spectral analysis of the flare hard X-ray emission

The M1.8 solar flare of 20 October 2002 (centered at 19° S, 23° W) started at about 14:21 UT in X-ray radiation in the NOAA Active Region 10163. Light curves of HXR emission detected by RHESSI in the 3–50 keV range indicate clearly the presence of QPP (Fig. 1). The light curve of X-ray emission detected by GOES is much smoother and does not reveal pulsations. It may be so because RHESSI's detectors have much higher count statistics of X-rays than GOES's detectors do. Unfortunately, solar radio telescopes used could not detect the above-background flux of microwave emission at frequencies above 8800 MHz, not allowing us to study dynamics of the mildly-relativistic electrons in this flare. Thus, further we will concentrate only on the analysis of HXR emission detected by RHESSI.

Using the OSPEX package within the Solar Software, we made spectral analysis of HXR emission (from full-disk and selected areas of the flare region) detected by RHESSI in different time intervals during the flare. The implemented best-fit-technique clearly indicates that the energy spectrum of HXR emission has thermal and nonthermal components which are fitted well by the double power-law function (the break energy is in the 15–25 keV range; the power-law spectral indexes are between –9 and –4). The nonthermal component dominates the thermal one above the energy of about 10–15 keV.

Looking at the light curves of HXR emission, we can subdivide the flare into two fundamentally different phases: impulsive and decay phases. The impulsive phase consists of eight QPP of nonthermal emission (episodes (E)–(M) in Fig. 1) with duration of about 30–40 s, indicating several acts of energy release and electron acceleration. These pulses are clearly composed of shorter quasi-periodic sub-pulses with duration of about 15–25 s which coincide in time with pulses of thermal emission. The decay phase, which started after the maximum of thermal HXR emission (after interval (M) on Fig 1.), consists mainly of pulses of thermal emission with duration of 15–20 s, while the decaying flux of nonthermal HXR emission mainly below 25 keV is also still present (this is not shown in Fig. 1 for clarity). This may indicate that there was no significant energy release in the decay phase of the flare, while nonthermal electrons accelerated mainly in the impulsive phase were still trapped in "post-flare" loops.

The presence of oscillations in the light curves of the observed HXR emission is confirmed by their spectral analysis. Firstly, to remove low frequency spectral components, we subtract the running averaged signals smoothed over 20 or 60 s [$F_{20,\ 60}\ (t)$] from the 4-s RHESSI data [$F_4\ (t)$]. Further, the Lomb periodograms are calculated for normalized signals $dF(t)/F_{20,\ 60}(t)=[F_4(t)–F_{20,\ 60}(t)]/F_{20,\ 60}(t)$: 1) during the whole flare [Fig. 2(A)], in the impulsive [Fig. 2(C)] and decay phases [Fig. 2(E)] separately for thermal emission; 2) only in the impulsive phase for nonthermal emission (when there was statistically significant flux of X-rays above the RHESSI background level; Fig. 2(G, I)).

The power spectrum of the normalized light curve of thermal emission reveals statistically significant peak of about 16 s both in the impulsive and decay phases, but more pronounced in the decay phase [see Fig. 2(B, D, F)]. The power spectra of the normalized light curves of nonthermal emission reveal two significant peaks around 16 and 36 s. Averaging over 60 s has strengthened the statistical significance of the 36-s peak in the spectrum, while averaging over 20 s has strengthened the significance of the 16-s peak. Splitting of the peak near 16 s to two more narrow peaks may be related to the short duration of the analyzed data sets.

3.2 Imaging analysis of the flare region

Fig. 3 shows images of the flare region made in different wavelength bands and in different time intervals during the flare. The EIT/SOHO images made in the impulsive phase and just after the decay phase jointly with the analysis of MDI/SOHO magnetograms [Fig. 3(A–D)] clearly indicate two closely spaced systems of flare loops: in south-east (SE) and north-west (NW). Unfortunately, the EIT/SOHO cadence of about 12 minutes is not enough to investigate dynamics of this flare.

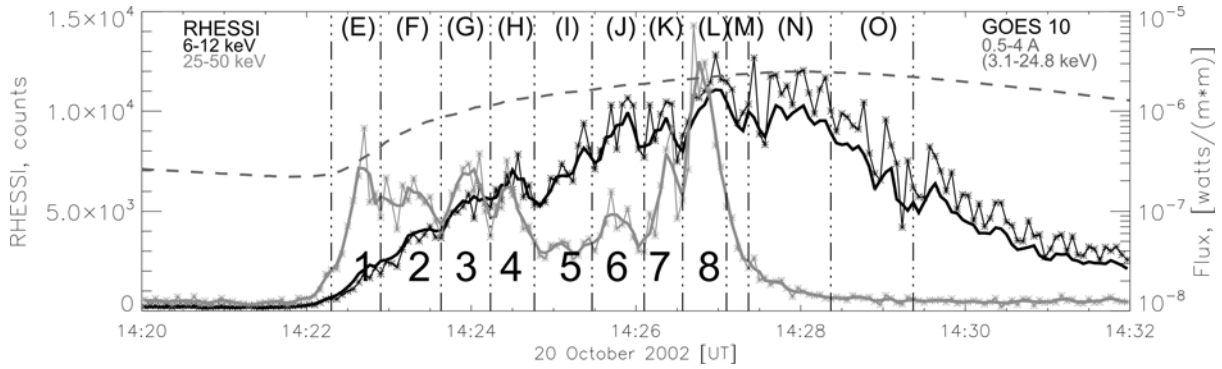

Fig 1. Time profiles of the full-disk X-ray emission observed by RHESSI's detectors 3, 4, 8 and XRS/GOES-10 during the solar flare under study. The time resolution of RHESSI data is 4 s (thin gray and black lines with asterisk; corresponding thick solid lines are the RHESSI data smoothed over 12 s; left vertical axis is in linear scale). The time resolution of the GOES flux data is 1 s (gray dashed line; right vertical axis is in logarithmic scale). The bold numerals indicate each QPP with time period of about 36 ss. Vertical dashed-dotted lines and bold letters in parentheses indicate time intervals in which RHESSI images (presented in Fig. 3 and denoted by the same letters) are made. The impulsive phase is between (E) and (M), and the decay phase is after (M).

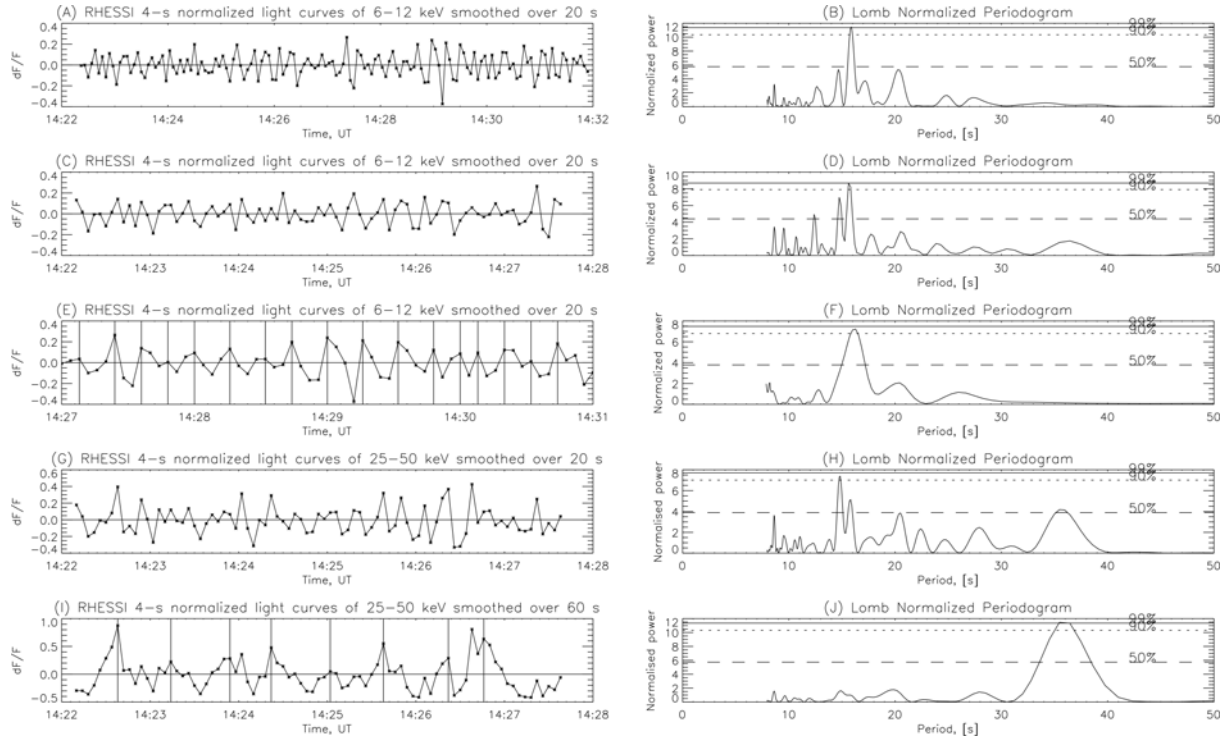

Fig 2. Panels (A), (C), (E), (G) and (I) show normalized 4-s light curves of HXR emission detected by RHESSI (F_4) in 6–12 (thermal) and 25–50 (nonthermal) keV energy channels in different time intervals of the 20 October 2002 solar flare: $dF/F=[F_4(t)–F_{20,\,60}(t)]/F_{20,\,60}(t)$, where $F_{20,\,60}$ is the running averaged by 20 and 60 s F_4, respectively . Panels (B), (D), (F), (H) and (J) show the normalized Lomb periodogram calculated for dF/F showed on the Panels (A), (C), (E), (G), (I), respectively. The 50, 90 and 99 % confidence levels are plotted by horizontal dashed, dotted and solid lines, respectively. Time profiles of thermal HXR emission, in particular in 6–12 keV range, reveal oscillations with the main period of about 16 s both in the impulsive and decay phases of the flare. The signal is more periodic in the decay phase. Time profiles of nonthermal HXR emission, in particular in 25–50 keV range, reveal two oscillation periods of 14–16 and 36–37 s.

To examine spatial evolution of thermal and nonthermal X-ray sources during the impulsive and decay phases, we reconstruct RHESSI images using the CLEAN and Pixon algorithms. Detectors 3–8 are used. Several series of images integrated over 8, 12,…, 60 s are obtained in different energy ranges and for different time intervals. We mainly work with 5(6)–10(12) keV (thermal X-ray sources) and 25–50 keV (nonthermal sources) images.

Fig. 3 (E–O) shows the morphology and dynamics of the flare region in X-rays. It is seen that early in the impulsive phase (up to about 14:25 UT) there were two clearly separated systems of flare loops (in south-east and north-west), whose positions coincided well with the loop systems SE and NW visible in EIT images. These loop systems were not independent. We calculate time profiles of thermal HXR flux at 6–12 keV both from the SE and the NW systems in the

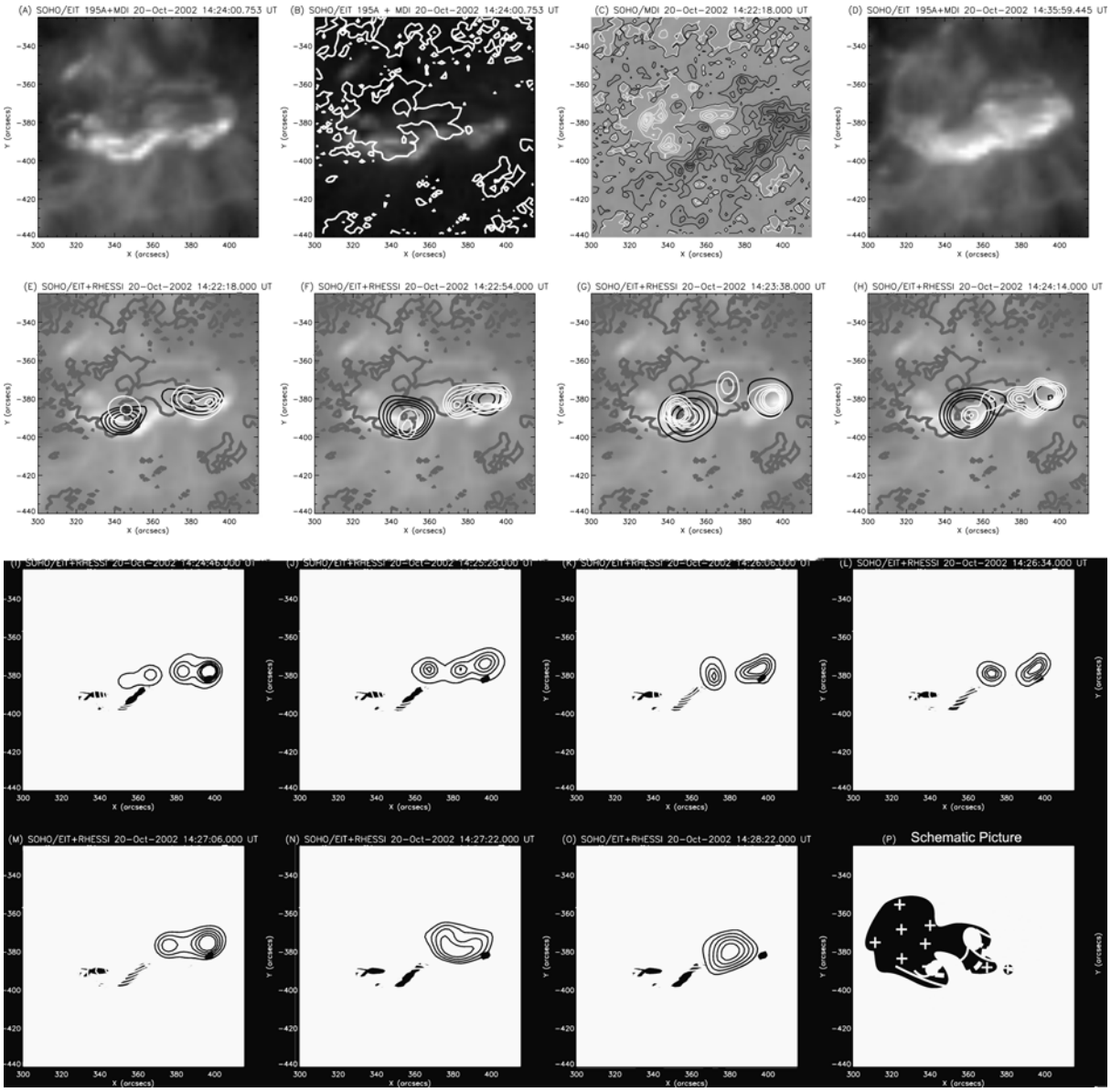

Fig 3. Images of the 2002 October 20 solar flare made in different spectral ranges of electromagnetic emission and different time intervals (projection on the photosphere; start time of each image is shown above). (A), (D): the EIT/SOHO images at 195 A made in the impulsive phase and just after the decay phase of the flare, respectively. (B): the EIT running-difference 195 A image. White lines indicate the 0 gauss isocontour (i.e., the magnetic inversion line) of the MDI photospheric magnetogram made in the impulsive phase. (C): the MDI magnetogram of the flare region overlaid by the isocontours at levels of +/–(10, 310, 610, 910, 1210, 1510) gauss (white and black lines). (E)–(O): the gray-color images are the same EIT 195 A image as shown in (A), but using another color palette for the clarity. Gray thick lines are the isocontours of MDI magnetogram at levels of +10 gauss indicating the magnetic inversion lines. Black and white lines are the RHESSI 5–10 keV and 25–50 keV contours (30, 40… 90 %) indicating thermal and nonthermal HXR sources, respectively. The RHESSI images shown in panels (E)–(O) were made for appropriate time intervals marked by the same letters in Fig. 1. (P): sketch of the flare region. The photospheric line-of-sight magnetic field of positive/negative polarities is shown by white/grey colors (+/– signs). Black solid lines, "SE" and "NW" designations indicate two systems of flare loops which interact through the oscillating thick gray dashed line (36-s periodicity). Thick black dashed line indicates the oscillating flare loops in the NW system (16-s periodicity). Black ellipses indicate the sources of nonthermal HXR emission (mainly in the footpoints of the flaring loops).

14:22:48–14:25:20 UT interval (when two systems were clearly separated), which we split into sub-intervals of 12 s to make time series of X-ray images. To calculate the HXR flux from each system we employ two circular integration regions with radius of 15 arcsecs for each system on each image. It turned out that fluxes of thermal HXR emission calculated from two separate systems were strongly correlated.

The space between two flare loop systems was gradually filled with thermal HXR radiation after about 14:25 UT (before commencement of the decay phase), indicating the presence of magnetic loops which could connect the SE and NW systems. The SE system and the space between two systems became practically invisible in HXR emission against the background of the bright NW source in the decay phase, possibly due to

the much stronger emission from the NW system and the limited dynamic range of RHESSI observations. Only the NW system was clearly observed in thermal HXR in the decay phase. Unfortunately, it is impossible to make spatially resolved analysis of the flare oscillations in thermal HXR emission because of the low spatial resolution of RHESSI.

Morphology of nonstationary nonthermal HXR sources located mainly in the footpoints of different flare loops also confirms the presence of two flare loop systems before about 14:25 UT. The sources of nonthermal HXR emission almost completely disappeared in the SE system after 14:25 UT [Fig. 3 (J, K)], while two footpoint-like nonthermal HXR sources in the NW system became stationary. Nonthermal HXR radiation filled the whole NW loop system, not only its footpoints, in the decay phase [Fig. 3 (M, N, O)]. This might have been caused by the trapped nonthermal electrons in these overdense loops.

4. Discussion

Based on the analyzed observational data, we can propose a rough scenario of the flare [see Fig. 3 (P)]:

(A) In the impulsive phase of the flare, energy was released and electrons were accelerated by successive acts with the average time period of about 36 s in different parts of two spatially separated and interacting loop systems of the flare region. These loop systems may interact through the connecting loop near both ends of which they are located. We established two observational evidences that these flare systems were linked: 1) fluxes of thermal HXR emission from these systems were strongly correlated; 2) the formation of the loop-type structure in the space between these systems was observed in thermal HXR emission. The question arises, is it possible to interpret the observed 36-s quasi-periodicity (P_{36}) of energy release in two different flaring systems by the MHD oscillations in the connecting loops? Indeed, it has been concluded from the imaging observations of another flare event that oscillations of even nonflaring transequatorial loop may be responsible for QPP of HXR emission observed simultaneously from two different active regions located at both ends of this loop [14].

We can roughly estimate the length of the connecting loops as $20 \le L_c \le 40$Mm and thus the required phase speed of a fundamental standing mode: $V_{PH}=2L_C/P_{36}$ or $1100 \le V_{PH} \le 2200$ km/s. This speed is consistent with those of the fast magnetoacoustic kink modes that were directly observed in coronal loops in the EUV emission ([1, 6] and references therein)! Implementing the imaging spectroscopy technique to the RHESSI HXR data allowed us to estimate the emission measure of different parts of the flare region. Hence, using the observed volumes of each flaring system and of the connecting loops, we managed to roughly estimate the averaged electron plasma densities in them: $10^{10} \le n_e \le 10^{11}$см$^{-3}$. Thus, the Alfvén speed in the connecting loops is $7B \le V_A \le 22B$ km/s, where B is magnetic field in gauss inside these loops. Thus, if $B \approx 100$ G (which is a reasonable value), we obtain $700 \le V_A \le 2200$ km/s that is very close to the estimated V_{PH}! Therefore, we conclude that the observed 36-s periodicity actually may be caused by the fast MHD oscillations in the connecting loops. The physical mechanism proposed in [8] is a good candidate to explain quasi-periodic spatial fragmentation of energy release in the impulsive phase of this flare. Multiple null-points might actually have existed in this flare region because of its complex topology: several inclusions of magnetic field of opposite polarity were seen on the magnetograms.

(B) During the first explosive acts of energy release, the MHD oscillations, probably global sausage modes, with time period of 16 s might have been excited in flaring loops of the NW system.

(C) These oscillations were maintained by the subsequent acts of energy release in the impulsive phase and were damped in the decay phase of the flare. We conclude that 16-s oscillations were excited only in the NW system but not in the SE system just because the NW system was more stationary and retained its loop-like configuration in the decay phase, when QPPs of thermal HXR emission were still observed but the SE system was no longer visible in HXR emission. The estimated lengths and plasma densities of the flaring loops in the NW system are $25 \le L_{NW} \le 35\ Mm$ and $10^{10} \le n_e \le 10^{11}\ cm^{-3}$, respectively. These physical parameters agree well with the same parameters found in [11] where 16-s quasi-periodic pulsations of microwave emission observed with the Nobeyama Radioheliograph were successfully interpreted in terms of the global sausage mode of oscillating flare loop. Thus, by analogy, we can also interpret the observed 16-s QPP of HXR emission by the global sausage mode excited in loops of the NW system. Moreover, the sausage mode must have been accompanied by perturbations of plasma density. Hence, this mode of oscillations would have quasi-periodically modulated thermal HXR emission. This is what we observed both in the impulsive and decay phases of the flare. The decay phase was not accompanied by significant energy release, so we clearly observed the damping of oscillations. Contrary to that, in the impulsive phase there were multiple explosive acts of energy release, which might have intermittently re-excited oscillations.

It is interesting to note that 16-s periodicity of nonthermal emission has already been observed in other solar flares [11, 15]. Perhaps, this is a typical period of the global sausage oscillations in flare regions [15]. The 36-s periodicity of HXR emission was also found in many solar flares [16].

Despite the above arguments, we are aware that the proposed flare scenario based on MHD oscillations of magnetic loops in a flare region may not be true. Oscillations of flaring loops itself were not detected directly using imaging observations, though this might have been because of observational limitations.

Acknowledgments

IVZ is grateful to organizers of the Baikal Young Scientists' International School for Fundamental Physics (2009), especially to Perevalova N.P., for providing accommodation and for the informational support. This work was partially supported by the Russian Foundation for Basic Research, grants No. 07-02-00319, 09-02-16032.

REFERENCES

1. Aschwanden M.J. Physics of the Solar Corona, Chichester, UK, 2009.
2. Vorpahl J.A. The triggering and subsequent development of a solar flare // ApJ. 1976. V. 205. P. 868.
3. Sakai J.-I., de Jager C. Solar flares and collisions between current-carrying loops // SSR. 1996. V. 77. P. 1.
4. Grigis P.C., Benz A.O. The evolution of reconnection along an arcade of magnetic loops // ApJ. 2005. V. 625. P. L143.
5. Aschwanden M.J. Review of coronal oscillations – An observer's view // NATO ASI Series. 2003. V. 124. P. 215.
6. Nakariakov V.M., Verwichte E. Coronal waves and oscillations // Living Rev. Solar Phys. 2005. V. 2 (3).
7. Zimovets I.V., Struminsky A.B. Imaging observations of quasi-periodic pulsatory nonthermal emission in two-ribbon solar flares // Solar Phys. 2009. V. 258. P. 69.
8. Nakariakov V.M., Foullon C., Verwichte E., Young N.P. Quasi-periodic modulation of solar and stellar flaring emission by MHD oscillations in a nearby loop // A&A. 2006. V. 452. P. 343.
9. Brown J.C., Hoyng P. Betatron acceleration in a large solar hard X-ray burst // ApJ. 1975. V. 200. P. 734.
10. Zaitsev V.V., Stepanov A.V. On the origin of the hard X-ray pulsations during solar flares // Sov. Astron. Lett. 1982. V. 8(2). P. 132.
11. Nakariakov V.M., Melnikov V.F., Reznikova V.E. Global sausage modes of coronal loops // A&A. 2003. V. 412. P. L7.
12. Asai A., et al. Periodic acceleration of electrons in the 1998 November 10 solar flare // ApJ. 2001. V. 562. P. L103.
13. Inglis A.R., Nakariakov V.M. A multi-periodic oscillatory event in a solar flare // A&A 2009, V. 493, P. 259.
14. Foullon C., Verwichte E., Nakariakov V.M., Fletcher L. X-ray quasi-periodic pulsations in solar flares as MHD oscillations // A&A. 2005. V. 440. P. L59.
15. Inglis A.R., Nakariakov V.M., Melnikov V.F. Multi-wavelength spatially resolved analysis of quasi-periodic pulsations in a solar flare // A&A. 2008. V. 487. P. 1147.
16. Lipa B. Pulsations in solar hard X-ray bursts // Solar Phys. 1978. V. 57. P. 191.

Институт космических исследований (ИКИ) РАН, Москва